This is a “preproof" accepted article for Journal of Glaciology. This version may be subject to change during the production process. 10.1017/jog.2025.15

Holocene hydrological evolution of subglacial Lake Snow Eagle, East Antarctica implied by englacial radiostratigraphy

AUTHORS:

Shuai Yan[1,2,*], Michelle R. Koutnik[2], Donald D. Blankenship[1], Jamin S. Greenbaum[3], Duncan A. Young[1], Jason L Roberts[4], Tas van Ommen[4,5], Bo Sun[6], Martin J. Siegert[7]

AUTHORS AFFILIATIONS:

1, University of Texas, Institute for Geophysics, Austin, USA
2, University of Washington, Department of Earth and Space Sciences, Seattle, USA
3, Scripps Institution of Oceanography, Institute for Geophysics and Planetary Physics, La Jolla, USA
4, Australian Antarctic Division, Kingston, Australia
5, University of Tasmania, Hobart, Australia
6, Polar Research Institute of China, Shanghai, China
7, University of Exeter, Penryn, Cornwall, United Kingdom
*: Corresponding author, contact at: syan94@uw.edu

ABSTRACT

A major subglacial lake, Lake Snow Eagle (LSE), was identified in East Antarctica by airborne geophysical surveys. LSE, contained within a subglacial canyon, likely hosts a valuable sediment record of the geological and glaciological changes of interior East Antarctica. Understanding past lake activity is crucial for interpreting this record. Here, we present the englacial radiostratigraphy in the LSE area mapped by airborne ice-penetrating radar, which reveals a localized high-amplitude variation in ice unit thickness that is estimated to be approximately 12 kyr old. Using an ice flow model that simulates englacial stratigraphy, we investigate the origin of this feature and its relationship to changes in ice dynamical boundary conditions. Our results reveal that local snowfall redistribution initiated around the early Holocene is likely the primary cause, resulting from a short-wavelength (~10km) high-amplitude (~20m) ice surface slope variation caused by basal lubrication over a large subglacial lake. This finding indicates an increase in LSE water volume during the Holocene, illustrating the sensitivity in volume of a major topographically-constrained subglacial lake across a single glacial cycle. This study demonstrates how englacial stratigraphy can provide valuable insight into subglacial hydrological changes before modern satellite observations, both for LSE and potentially at other locations.

INTRODUCTION

Antarctic subglacial hydrology networks are highly sensitive to the surface form of the Antarctic Ice Sheet (Wright and others, 2008). Changes in ice surface elevation and surface slope throughout glacial cycles have the capacity to significantly change the configuration of ice flow, even in central ice-sheet regions (Siegert and others, 2004) and, because of this, to change subglacial hydrological networks (i.e., subglacial water flow direction, location of subglacial lakes, catchment area, etc.). As key components of subglacial hydrological networks, we can assume that subglacial lakes too may be subject to changes over glacial cycles, including their volume. Subglacial hydrological networks can impact the overlying ice flow by changing the basal friction and ice bottom elevation (Livingstone and others, 2022). Subglacial drainage has also been shown to modulate the basal melting pattern of ice shelves (e.g., Wei and others, 2019; Pelle and others, 2023).

Understanding the close interaction between ice sheets and subglacial hydrology systems is, therefore, critical for accurately simulating the behavior of ice sheets and ice shelves throughout glacial cycles in order to understand ice-sheet evolution.

Recent airborne geophysical surveys coordinated by the second International Collaborative Exploration of the Cryosphere through Airborne Profiling (ICECAP2) initiative confirmed the existence of a large subglacial lake, Lake Snow Eagle (LSE), in the interior of Princess Elizabeth Land (PEL), East Antarctica (Yan and others, 2022) (Fig. 1). LSE is located in the upstream part of an extensive subglacial canyon network, whose orientation is orthogonal to the ice flow direction near LSE and likely connects to the coastal area of PEL (as estimated by Jamieson and others (2016) based on satellite-based observation of the ice surface, assuming the large-scale feature on the ice surface reflects subglacial topography) (Fig. 1). Such subglacial channels could serve as efficient subglacial water pathways, making LSE potentially connected to the surrounding and downstream subglacial hydrology networks. Therefore, the drainage of LSE could influence the downstream subglacial hydraulic conditions and impact the flow dynamics of the downstream ice.

Figure 1 near here

Geophysical inversion of airborne gravity data collected by ICECAP2 indicate the existence of a sediment layer up to over 200 meters thick at the bottom of LSE (Yan and others, 2022). Given the low expected sedimentation rate, such a substantial sediment layer likely holds a valuable and rarely available record of geological and environmental changes in the interior of East Antarctica (Kennicutt and others, 2019; Yan and others, 2022). One critical reference for future analysis and interpretation of this sediment record is the past evolution of LSE; for example the draining and refilling of lake water and changes in the catchment area. Because the migration of subglacial water (i.e., subglacial lake drainage and filling events) could induce localized changes in ice surface elevation, such events can be monitored by satellite observations if the water drainage volume is large enough (e.g., Fricker and others, 2007). One approach to constraining these observations prior to the satellite record is to directly access these sediments to observe laminations (Siegfried and others, 2023), however at a depth of over 3.5 km, LSE is a challenging target for access and sampling, and without expected radiogenic,

biological or satellite-detected elevation change constraints on timing, a sediment based approach alone would seem difficult.

Fortunately, englacial radiostratigraphy can retain valuable information about the history of the ice sheet including past ice flow reconfiguration (e.g., Beem and others, 2018), paleo-accumulation patterns (e.g., Waddington and others, 2007; Leysinger Vieli and others, 2011; Cavitte and others, 2018), and basal melting patterns (e.g., Ross and Siegert, 2020). In particular, time-varying boundary conditions experienced over limited parts of the ice sheet, for example transitions from frozen to melting at the bed, may be imprinted on layer shapes. Therefore, englacial stratigraphy offers a unique opportunity to gain insight on the past evolution of LSE. In this study, we combine the englacial radiostratigraphy in the LSE area with a numerical ice flow model that simulates englacial stratigraphy to investigate the hydrological evolution of LSE. Such knowledge is important for understanding the sedimentary record within LSE and, more broadly, past changes in the PEL sector of the East Antarctic Ice Sheet.

METHODS

Airborne ice-penetrating radar sounding and englacial stratigraphy

Ice-penetrating radar systems have been used to advance our understanding of the cryosphere for over five decades (see Schroeder and others (2020) and references therein). Such radar systems provide high resolution measurements of subglacial topography and ice sheet thickness (e.g., Cui and others, 2020), as well as valuable insights on englacial structure and subglacial hydraulic conditions (e.g., Schroeder and others, 2013; Beem and others, 2018; Yan and others, 2022) (Fig. 2, Fig. S1, and Fig. S2). The airborne survey platforms deployed in ICECAP2 seasons are equipped with an ice penetrating radar based on the HiCARS2 system developed by University of Texas Institute for Geophysics, which is a coherent, 60 MHz ice-penetrating radar system with 15 MHz of bandwidth (Peters and others, 2005; Young and others, 2011; Cui and others, 2018). After pulse-compression and synthetic aperture radar (SAR) processing (Peters and others, 2007), this system provides a vertical resolution of 8.5 meters in ice and an along-track resolution of 44 meters (Cavitte and others, 2018). The radar data used in this study was collected in PEL over four field campaigns (2016-19) through the ICECAP2

initiative. To expand the stratigraphic chronology of the region, these radar surveys were designed to connect to the pre-existing radar datasets with internal layers dated from ice-core intersections in the Lake Vostok and Dome C regions (Fig. 1).

Figure 2 near here

In this study, we use internal reflecting horizons (IRHs) to infer past evolution of the ice sheet. IRHs in ice-penetrating radar sounding are caused by variations in electric conductivity and permittivity across the ice column, due to changes in ice fabric, density, and acidity (Wrona and others, 2018; Bingham and others, 2024). Continuous IRHs are generally considered isochronous (i.e., resulting from layers of snow deposited on the ice sheet surface around the same time) (e.g., Eisen and others, 2006; Ashmore and others, 2020; Elsworth and others, 2020). Nine IRHs of interest in the LSE area (referred to as PEL_EDC_IRH01-09) are traced using the DecisionSpace Geosciences 10ep software package (Fig. 2, Fig. S1, and Fig. S2), which contains semi-automatic tracing algorithms and enables continuous IRHs tracing across transects (Cavitte and others, 2021). These nine IRHs are selected because they cover the depth range where a disruption in the englacial stratigraphy is observed, as well as their overall continuity. While a series of additional reflections are also visible in the deeper portion of the ice column, those reflections are vulnerable to disruptions when the ice flows over rough terrain and are therefore largely discontinuous and difficult to trace. The thickness of ice units between traced IRHs are then calculated assuming a constant electromagnetic velocity of 168.5 m μs^{-1} in ice (Cavitte and others, 2016).

In addition to the aforementioned nine IRHs traced in the LSE area, we extend six of the dated IRHs in Cavitte and others (2021) from the Dome C area to PEL, which were dated by referencing the AICC2012 chronology (Bazin and others, 2013; Veres and others, 2013) (Fig. 3b). With these dated IRHs providing a reference, and assuming the age of 0 ka (present) for the ice sheet surface, we use the Dansgaard and Johnsen age-depth model to estimate the age of the nine aforementioned undated IRHs traced in the LSE area (Dansgaard and Johnsen, 1969). The Dansgaard-Johnsen model is a one-dimensional ice flow model that assumes a shear layer above the bottom of the ice column capped by a non-shear layer. The horizontal ice flow velocity in the bottom shear layer is assumed to be proportional to the elevation above bed, while the horizontal ice flow velocity in the top non-shear layer is assumed to be constant and elevation-independent.

Because the thickness of the shear layer is unknown for our study area, we construct four models to represent possible locations for the shear-layer boundary: (1) below the 96 ka reflection, (2) between the 96 ka reflection and the 82 ka reflection, (3) between the 82 ka reflection and the 73 ka reflection, and (4) above the 73 ka reflection. Models with different assumptions of shear-layer boundary depth appear to yield similar results, as shown in Fig. 3c.

Figure 3 near here

We use the Dansgaard-Johnsen model to constrain the age-depth profile at 91 selected sites in south-eastern PEL (Fig. 3a), the statistics of which is then used to estimate the age of the traced englacial reflections. These locations were selected based on three criteria: (1) most of the traced englacial reflections from the LSE area and dated englacial reflections from the Dome C area are identifiable and continuous, (2) basal roughness is relatively low, which enables us to neglect the influence of rough terrain, and (3) proximity to ice divide. These criteria increase the likelihood that the assumptions underlying the 1-D the Dansgaard-Johnsen model are met.

We acknowledge that the 1-D Dansgaard-Johnsen model is a relatively simple tool for estimating the age-depth profile and relies on several key assumptions about ice flow conditions. Specifically, this approach involves averaging the surface accumulation rate over the entire time span represented by the ice column. While this simplification provides a first order estimate of the age of the traced IRHs, it may introduce inaccuracies, particularly in regions where the surface accumulation rate has varied significantly over time. Therefore, if future studies are able to provide constraints on past accumulation rate changes in the study area, incorporating this variability into the age-depth model will be essential for improving the accuracy of age estimations.

Ice flow model

In this study, we use a 2.5-D ice flow forward model that allows for varying boundary conditions to understand the evolution of LSE (Koutnik and Waddington, 2012). This model can simulate the geometry of englacial horizons of prescribed ages, which then can be compared to the observed IRHs. The ice flow model represents a vertical 2-D cross section of the ice sheet from the surface to the bed, with an additional half dimension accounting for transverse strain rate

along the ice flow direction (Fig. 1a). The model has a limited domain, constrained to the interior of the ice sheet, extending from the upstream ice divide to downstream of LSE where the radar measurement profile ends. By including the upstream ice divide in the model domain, the upstream boundary condition is a zero-flux condition and any influences from the surface and bed conditions upstream are advected to the vicinity of LSE and represented in the simulated stratigraphy.

The model incorporates general information about the full-domain response of the ice sheet through response functions that scale how the limited portion of the ice sheet responds to changes in accumulation and ice flux over time (Koutnik and Waddington, 2012). Boundary conditions for the ice flow model and the values we prescribe in the model include: (1) bed elevation, which we obtain from measurements by airborne radar sounding (Cui and others, 2020); (2) flow band width, accounting for transverse strain rate along the ice flow direction, which we derive by tracing ice velocity divergence along the ice-flow direction, with ice-surface velocity from MEaSUREs InSAR-Based Antarctic Ice Velocity Map, Version 2 (Rignot and others, 2017); (3) geothermal flux, which is estimated from satellite magnetic data by Maule and others (2005); (4) surface accumulation rate (varying spatially between ~4 to 6 cm/yr) and mean-annual surface temperature (varying spatially between -40 to -30 ^{o}C), which were estimated based on values from the RACMO2 model (van Wessem and others, 2018). In this model study, we assume that the surface elevation has been similar to the modern values over the past 23 ka of the model run.

Our ice flow model uses the Shallow-Ice Approximation (SIA) to describe the ice-flow field (Cuffey and Paterson, 2010), except that we assume plug flow over LSE when the lake is active with the ice flowing at a column-uniform rate that is less than the surface velocity; the plug-flow velocity over the lake is a tunable parameter. The horizontal resolution of the model is chosen to be 1000 m, which reasonably represents the stratigraphy and is necessarily efficient, and the vertical resolution is non-dimensionalized by the ice thickness to be 0.002 (approximately 5-7 m along the domain when dimensionalized). The time stepping in the model runs is 100 years, but particle tracking through the gridded velocity field is done at finer resolution using an interval stepping of 1000 for all modeled IRHs.

By integrating the modeled velocity field, the paths of ice particles deposited on the surface over time can be used to calculate the englacial stratigraphy. This

modeled englacial stratigraphy is then compared with the observed englacial stratigraphy obtained by radar sounding, similar to the iterative evaluation process in Koutnik and others (2016). A more detailed description of the ice flow model can be found in the Supplementary Materials (Supplementary Note #1).

RESULTS

Englacial stratigraphy over the LSE area

In this study, nine continuous englacial reflections within the top half of the ice column are traced by semi-automatic tracing algorithms across the LSE area and towards south-eastern PEL (Fig. 2), and their age estimations are shown in Table 1.

Table 1 near here

We observe a change in the englacial radio-stratigraphy pattern in the upper ice column over LSE. While the thickness of the ice units between IRHs are relatively constant upstream of LSE (left-hand side in Fig. 2, and grid south in Fig. 4), distinct short spatial wavelength, high amplitude spatial variations in ice unit thickness are present in the upper ice column over LSE (Fig. 2 and Fig. 4). The most prominent variation is observed in the ice unit whose formation age is estimated to be between 9.5 ka and 12 ka, where the thickness of this unit varies by more than 150 meters across horizontal along-flow distance of 10 kilometers (Fig. 4). The horizontal extent and location of this anomalous thickness variation corresponds well with LSE (Fig. 2 and Fig. 4), while the thickness of this ice unit stays relatively constant elsewhere in the study area. This anomalous stratigraphic disruption observed above LSE indicates past changes in ice-flow dynamics resulted in such a distinct signature being recorded in the englacial stratigraphy. The strong spatial correspondence between this stratigraphic disruption and LSE implies a connection between ice-flow changes and the subglacial lake.

Figure 4 near here

Qualitative analysis of the change in englacial stratigraphy over LSE

To investigate the potential processes that may contribute to the observed disruption of englacial stratigraphy in the vicinity of and across LSE described in

the previous section, we consider factors and processes that can potentially alter the englacial stratigraphy, including:

(a) Subglacial topography. LSE is located inside a subglacial canyon, whose orientation is orthogonal to the regional ice flow direction (Jamieson and others, 2016; Yan and others, 2022). The canyon's extreme topographic relief - more than 1000 meters over just a few kilometers - can significantly disrupt the ice flow, particularly near the base, and alter the shape of the IRHs. The imprint of subglacial topography on englacial stratigraphy tends to correspond with the along-flow derivative of topography (e.g., Ross and Siegert, 2020), typically being vertically-continuous propagating from bottom upwards where the impact has a similar amplitude in adjacent ice layers. The imprint of subglacial topography is also expected to be more pronounced for the IRHs closer to the ice-rock interface compared to the IRHs near the ice surface.

(b) Climate-controlled changes in the rate and pattern of surface accumulation throughout the time span that is covered by the traced IRHs in the LSE area (e.g., Leysinger Vieli and others, 2011), whose imprint would have a relatively long horizontal span. For example, the reconstructed paleo-accumulation rate at Dome C by Cavitte and others (2018) shows variation with a spatial wavelength on the order of hundred kilometers.

(c) Past ice flow reorganization, whose imprint tends to be horizontally continuous and has a long-spatial-wavelength imprint on the englacial stratigraphy (e.g., Beem and others, 2018) and, vertically, can only be observed in the IRHs formed prior to and around the time of the reorganization.

(d) Changes in ice-flow rate due to subglacial water storage that decreases the basal friction in the vicinity of the subglacial water body (e.g., Sergienko and Hulbe, 2011; Gudlaugsson and others, 2016). Similar to factor (a), the imprint from sliding over basal water tends to be vertically continuous, propagating from bottom upwards where its horizontal extent would correlate with the subglacial water body, and is only present when the basal non-friction zone is of a sufficient area (e.g., Sergienko and Hulbe, 2011; Gudlaugsson and others, 2016).

(e) Basal melting and freezing, which can be present at the ice-water interface above subglacial lakes (e.g., Vieli and others, 2007; Filina and others, 2008; Leysinger Vieli and others, 2018). For the imprint of basal melting and freezing, its horizontal span of IRH shape is confined primarily to the melting/freezing spots (e.g., Ross and Siegert, 2020), while vertically its imprint can be present across the entire ice column.

(f) Redistribution of surface snowfall by the combination of surface wind and surface slope break (e.g., Grima and others, 2014), whose imprint tends to have a short horizontal span that correlates to local changes in surface slope (e.g., Verfaillie and others, 2012; Guo and others, 2020). Vertically, the imprint would be mostly confined within the IRHs that were formed during the time period when such redistribution was present.

The disruption of englacial stratigraphy above LSE is only present in the upper half of the ice column (Fig. 2, Fig. 4, Fig. S1, and Fig. S2). Horizontally, in the along-flow direction, this disruption extends over a similar distance as the along-flow width of LSE and its hosting subglacial canyon, with a span around ten kilometers (Fig. 2, Fig. 4, Fig. S1, and Fig. S2). Across the ice flow direction, the width of this disruption is comparable to the across-flow width of LSE, which is around 40 kilometers (Fig. 2, Fig. 4, Fig. S1, and Fig. S2). After comparing these characteristics against those outlined above for process (a), (b) or (c), it appears that these specific mechanisms are less likely to be the primary driver of the observed disruption. We cannot entirely dismiss their influence, as more complex interactions may still play a role. Fully constraining the impact of these processes, however, is particularly challenging due to the limited understanding of the area's complex topographic setting and the past changes in ice flow and climate conditions. As the primary goal of this study is to identify the primary cause for the anomalous stratigraphic disruption observed over LSE, we choose to focus on the other potential mechanisms and apply a simplified ice flow model to quantitatively assess their impact on the englacial stratigraphy, providing a more detailed understanding of the observed stratigraphic disruption.

Quantitative analysis of the irregular englacial stratigraphy at LSE

To systematically investigate the potential source of the irregular stratigraphy, we assess the impact of different processes by tracking how the modeled layers change as a function of combinations of different model-parameter values representing those processes, and compare the modeled IRHs shape and depth to the radar observation.

(1) Base model setup

To evaluate the parameter choice and model setup, we first build a "base run" with the modern bed elevation as measured from radar sounding, without water fill of the subglacial canyon, basal melting, basal sliding, or surface accumulation redistribution over LSE (Fig. 5a-b). The mismatch shown in Fig. 5 is calculated by comparing the modeled depth and the observed depth of each IRH, where positive mismatch means that the modeled IRH is deeper than observed.

To evaluate model fit, we calculate the root-mean-square (RMS) mismatch between the modeled and observed stratigraphy across the model domain. A lower RMS indicates a better overall fit. Additionally, we need to consider the tolerance value in order to evaluate our model fits, as for this study we seek the minimum mismatch but need to consider that the data have uncertainties. The modeled IRH depth is affected by the inferred IRH age uncertainty. By comparing the depth difference between IRHs with an age difference of around 1 kyr, it appears that a reflection age difference of 1ka induces a depth difference of around 65 meters. As the standard deviations for IRH age estimation for most traced IRHs are around 1 kyr, we treat this 65-meter value as a tolerance for fitting IRHs with our model. We refer to model setups with an RMS mismatch smaller than 65 meters as "accepted setups", but we do not rank these "accepted setups " or interpret parameter combinations from a single accepted model. If this was set up as a formal inverse problem, or if additional constraints on the ages of the traced IRHs were available through direct or indirect approaches, we could more rigorously consider data uncertainties and work towards finding the "best" set of model parameters within these uncertainties that avoids overfitting the data (e.g., Gudmundsson, 2011). For this study we seek to constrain characteristics of model setups that minimize the mismatch to the observations, and to support future work that can more robustly evaluate inferences about specific parameters and/or combinations of parameters in a different modeling framework.

For the base model setup, the mismatch RMS across all nine traced IRHs within the shown model domain is 133 meters. Upstream of LSE (the left half of

the model domain shown in Fig. 5), the mismatch between simulated and observed englacial stratigraphy is within the order of inherited uncertainty from IRH age estimation (65 meters), which indicates that the model setup and parameter selection are reasonable. However, above and downstream of the lake, the modeled IRHs are over 300 meters shallower than the observation, and the short wavelength variation over the lake in the upper half of the ice column is not produced. This result indicates the need to incorporate additional processes into the model.

Figure 5 near here

(2) Impact of basal lubrication and basal melting

Next, we examine the impact of basal lubrication (by existence of a subglacial lake) and basal melting on the englacial stratigraphy. Previous studies have estimated the basal melting rate of other major subglacial lakes to range from centimeters per year to tens of centimeters per year (e.g., Siegert and others, 2000; Ross and Siegert, 2020). Since the contemporary basal melt rate of LSE is not constrained, we use this range as a starting point to assess the impact of basal melt on englacial stratigraphy. As a preliminary test, we impose plug flow and a basal melt rate of 0.1 m/yr in the model over the location of LSE, and then compare the modeled englacial layers to the observed layers (Fig. 5c-d). The mismatch RMS for this model setup is 90 meters. The modeled IRHs above LSE are deeper than those in the base run, due to the drawdown effect of basal melting, thereby resulting in a reduced mismatch. However, there remains a mismatch of approximately 300 meters over LSE, and the observed stratigraphic disruption above LSE is not adequately reproduced. This result indicates that while basal melting is or has been present over LSE, it is not the primary cause for the irregular englacial stratigraphy observed in the upper ice column over LSE.

(3) Impact of surface snowfall redistribution

Next, we proceed to explore the potential impact of surface snowfall redistribution that could be present in the LSE area. With a sufficient area of basal lubrication, the impact of basal sliding can propagate through the entire ice column, resulting in a distinctive localized high-amplitude variation of the ice surface slope. Such expression is observed for many major subglacial lakes (e.g., Filina and others, 2008), including LSE (Yan and others, 2022) (Fig. S8, and Fig. S9). While the overall ice surface slope in the area dips toward the grid north-east direction as the ice flows towards the Amery Ice Shelf, a local 20 m depression can be observed over the subglacial lake (Fig. S9). It has been shown that such localized variation

of surface slope is capable of redistributing surface snowfall (e.g., Sugiyama and others, 2012; Verfaillie and others, 2012; Grima and others, 2014). More specifically, short wavelength "breaks" in surface slope have been shown to induce a relatively significant increase in surface accumulation rate by redistributing surface snowfall. Both airborne radar sounding surveys and satellite based observations show such a surface feature is present over LSE (Yan and others, 2022), which indicates that topographic redistribution of surface snowfall could be present in the LSE area. Additionally, a study conducted by Das and others (2013) identified likely wind scour zones across East Antarctica based on surface slope, where scour zones are identified within 10 km of LSE. This finding suggests snowfall redistribution caused by the combination of wind scour and surface slope is likely present in the vicinity of LSE. Such a localized anomaly in surface accumulation can cause a short-wavelength variation in the ice unit thickness, and the impact of this process is expected to propagate from the ice surface downward in the ice column over time.

We note that it is not clear whether the ice surface slope break at the contemporary LSE location has been persistent across glacial cycles. Having such a large area of ice surface slope variation requires a large area of basal lubrication where basal shear stress is zero. Given that LSE is located in a deep subglacial canyon (Yan and others, 2022), any large area of basal lubrication would require that a substantial water volume fill the canyon hosting LSE. Subglacial lakes can refill and drain under the influence of the basal thermal conditions coupled to any dynamically induced changes in the overlying ice sheet slope (Livingstone and others, 2022). Therefore, it is possible that the surface accumulation anomaly caused by local snowfall redistribution has only existed for a limited amount of time. If so, its impact—short-wavelength variation in the ice unit thickness—can only be observed in the ice units formed when this process is present.

To assess the impact of this process, we impose a positive surface accumulation anomaly on the upstream lake edge in the ice flow model that is associated with the presence of subglacial lake. As a preliminary test, we first impose a 150% increase of net surface accumulation rate at the upstream edge of the lake. The crossflow extent of this snowfall redistribution is 34 km, which corresponds to the width of the stratigraphic disruption across the flow direction. In this preliminary test, the subglacial lake and the snowfall redistribution are assumed to be present for the entire modeled time period. This model setup with

the upstream surface accumulation anomaly produces a better fit to the observed englacial stratigraphy compared to the previous model setup, especially for layers in the upper half of the ice column over the lake (Fig. 5e-f). This finding indicates that snowfall redistribution associated with the presence of a subglacial lake might exist in the study area and could influence the shape of IRHs. The characteristics of this snowfall redistribution remains unconstrained and will be further investigated in the following section.

(4) Evaluating a wider range of parameter values

The model runs described above have demonstrated how various processes can alter englacial stratigraphy, through their representation as parameters in the model. We aim to further investigate the englacial layer impact of these processes by evaluating combinations of the five key model parameters that we have shown to affect the outcome of the model runs: (1) time duration of snowfall redistribution; (2) amplitude of surface snowfall redistribution; (3) spatial span of surface snowfall redistribution along the model profile; (4) basal melt rate over the lake; and (5) the plug flow velocity factor that is imposed over the lake.

We note that there can be trade-off effects among these parameters, and different parameter combinations could produce similar mismatches between the modeled and observed stratigraphy within the observational uncertainty. For example, both a prolonged snowfall redistribution duration coupled with a low snowfall redistribution amplitude, and a shorter duration paired with a higher amplitude, can produce similar matches to the observed stratigraphy. Due to the absence of direct measurements for these parameters, constraining each one independently of assumptions about the other parameter values can be challenging; the problem can be non-unique. Therefore, a goal of this study is to evaluate different parameter combinations and to establish the physical appropriateness of the parameter values required to fit the layer observations.

Ultimately, we conducted a suite of 1404 runs, evaluating the parameter space that covers all the possible combinations of parameters within the ranges listed in Table 2; i.e., 1404 parameter combinations with these ranges bounding our initial estimation of the parameter value. For this suite of runs, the time duration of snowfall redistribution is estimated to be between 3ka and 15 ka, extending beyond the estimated age of the ice unit where the abnormal thickness variation is observed (9.5ka - 12ka). We note that the time duration of snowfall redistribution is also used as the time duration of basal melting and plug flow over the lake, i.e.,

basal melt rate is set to be zero and plug flow is not enforced when snowfall redistribution is not present. These three factors are all caused by the presence of a major subglacial lake, therefore are set to be present or absent together. The amplitude of snowfall redistribution around LSE is not constrained by measurement; however, observations in other Antarctic regions where similar processes are observed suggest redistribution amplitudes can be as large as over 100% (e.g., Guo and others, 2020). Therefore, we consider a range of four values from 50% to 200%. Given that snowfall redistribution is primarily influenced by surface wind scour and ice surface slope break, it is reasonable to assume that the spatial extent of redistribution is comparable to the size of the ice surface slope break across LSE. Basal melt rates are estimated to range from centimeters to tens of centimeters per year, based on estimations for other major subglacial lakes in Antarctica (e.g., Filina and others, 2008; Thoma and others, 2009). The value range of the plug flow factor covers a wide range from 0.1 to 0.7, as we lack measurements of the velocity-depth profile of the LSE area.

Table 2 near here

Within this series of model setups, 21 parameter combinations produce a mismatch RMS value less than the aforementioned 65 meters threshold (Fig. 6, Fig. 7, Fig. S7, Table 3, and Table S1). As noted, we cannot reliably distinguish these setups as their mismatch falls into the margin of uncertainty. However, these 21 setups collectively represent the best fit achievable with our current understanding. Fig. 7 shows the parameter distribution of these 21 setups. The parameter values of the accepted combinations provide valuable constraints on the processes driving the stratigraphic disruption above LSE:

- The snowfall redistribution duration of all 21 accepted setups range between 5 to 11 kyr, with no durations falling outside this range yielding a mismatch RMS smaller than the 65-meter threshold (Fig. 7a). A snowfall redistribution with a duration within this range produce a thicker ice unit at the upper ice column without significantly changing the shape of the lower IRHs. Because snowfall redistribution is likely to be currently present above LSE, the duration of this process can offer information about its initiation time. Therefore, our result indicates that the snowfall redistribution in the

study area only started in the Holocene epoch and was not present prior to this period.

- All accepted setups implement snowfall redistribution amplitudes larger than 150% (Fig. 7b), and the spatial extent of snowfall redistribution in all but one of the accepted setups is 34 km (Fig. 7c), suggesting that a large area of strong snowfall redistribution is needed to produce the observed englacial stratigraphy.
- The modeling result shows all of the combinations implement a low basal melt rate of about 0.1 m yr^{-1} (Fig. 7d).
- Lastly, no distinct optimum is observed in the tested plug flow factor values (Fig. 7e). This result indicates that the shift from frozen bed to lubricated bed, and the consequential change in the englacial strain and stress fields, doesn't have a strong influence on the englacial stratigraphy in the upper ice column, which is expected for an area with low ice-flow velocity.

Figure 6 near here
Table 3 near here
Figure 7 near here

DISCUSSION

Holocene evolution of LSE

Our modeling suggests that the irregular englacial stratigraphy observed above LSE cannot be matched as well without a time-variant surface snowfall redistribution (Fig. 7). The surface snowfall redistribution is caused by the local ice surface slope variation above LSE, which is induced by the presence of a major subglacial lake and the resulting basal lubrication. Therefore, a potential driver for such time-variant snowfall redistribution can be subglacial drainage and refilling through time that can alter the water volume of LSE. The LSE bathymetry constrained by Yan and others (2022) reveals deep basins in the grid northeast part of the lake. This finding suggests that as the lake water volume increases, (i) along the ice flow direction, the area of basal lubrication would primarily expand

upstream, and (ii) across the ice flow direction, basal lubrication would predominantly extend toward the grid-west direction along the subglacial canyon. When the basal lubrication area reaches a sufficient size, the entire ice column can shift into plug flow, resulting in localized variations in ice surface slope over the lubricated area – this is observed as a localized ~20m depression of ice surface elevation over LSE (Fig. S8, and Fig. S9). This lake activation can lead to the local redistribution of surface snow, with a notable increase in the surface accumulation rate at the surface depression compared to the surrounding areas. This mechanism establishes a connection between the time span of surface accumulation anomaly and that of LSE's water volume reaching the present level. The modeling results show that the better fits occur when the surface accumulation anomaly begins only around the early Holocene (Fig. 7), which could indicate that LSE experienced a substantial increase of water volume at this time. While we cannot quantify the exact amount of this water volume increase, our modeling results suggest that prior to this era, the water volume was insufficient to generate an area of basal lubrication as widespread as present.

The Holocene increase of LSE water volume inferred in this study is likely a part of a larger scale evolution of the subglacial hydrological system in the interior of East Antarctica. The location and volume of subglacial lakes are determined by both subglacial hydraulic slope and subglacial topographic slope (Dowdeswell and Siegert, 1999; Wright and Siegert, 2011). Under the contemporary East Antarctic Ice Sheet (EAIS) configuration, the upstream catchment of LSE originates near Ridge B in central East Antarctica. However, since the Last Glacial Maximum (LGM), the EAIS has experienced significant changes in ice thickness and volume (e.g., Gowan and others, 2021), which could have induced substantial changes in subglacial hydraulic slope and water routing and resulted in subglacial water being stored in different locations than in the past (Wright and others, 2008). Additionally, the presence of sedimentary basins and groundwater systems in parts of Antarctica (e.g., Li and others, 2022; Gustafson and others, 2022), along with spatially heterogeneous subglacial thermal conditions (e.g. Shackleton and others, 2023), suggests that changes in water routing could significantly influence the degree of heat exchange that subglacial water experiences as it travels from upstream sources to downstream lake basins. This may alter the basal thermal conditions in downstream areas, potentially impacting the basal melt rate and even the stability of the ice sheet in those regions. The increase of LSE water volume in

the Holocene underscores the potential sensitivity of a major Antarctic subglacial lake to the change of glacial and climate conditions.

The hydrological evolution of LSE constrained in this study offers a critical reference for the future interpretation of the sedimentary record preserved at the lake bottom (Yan and others, 2022). Specifically, (a) changes in lake water volume and basal melt rate can alter lake circulation patterns, potentially redistributing sediments after their initial deposition (Filina and others, 2008); (b) change of upstream catchment could shift the source and composition of the sediment transported by subglacial water flow; and (c) lake filling could result in un-grounding of sediment, influencing its depositional environment and stability (Smith and others, 2018). These factors must be considered and evaluated when selecting the drilling site for lake access and interpreting the LSE sediment record in the future.

Our work opens up the potential for similar approaches to be applied to other large topographically-constrained subglacial lakes, enabling investigation of time-dependent volume change of very large subglacial lakes, thought previously to be isolated and stable (Dowdeswell and Siegert, 1999; Siegert, 2005). Several previous studies have utilized satellite observations to investigate the migration of subglacial water and the draining and filling of subglacial lakes (e.g., Wingham and others, 2006; Carter and others, 2011; Fricker and others, 2016), through the observed local-scale changes of ice surface elevation that cannot be attributed to other mechanisms. Such lakes are characterized by being largely unconstrained by basal topography, thus making them susceptible to modest glaciological changes (Siegert and others, 2014). This study differs from previous investigations, as it demonstrates volume change within a subglacial lake constrained well by deep basal topography. Extending from this work, a broader investigation could potentially provide valuable insights into the coupled evolution between Antarctic subglacial hydrology and the Antarctic Ice Sheet on centennial to millennial timescales, and not just across subglacial lakes.

While it is reasonable to assume that continental-scale ice sheet adjustment might lead to volume loss/gain in large subglacial lakes, this paper provides the first evidence of it. Previously, the morphological signature of colossal volumes of basal water evacuated from the East Antarctic Ice Sheet has been found in the western Dry Valleys; the so-called ‘Labyrinth’ and associated landforms that formed in the Miocene ~14 Ma (Denton and Sugden, 2005). Such morphology,

involving km-scale channels cut into bedrock, appear far too big to be the result of small ‘active’ lake outburst. Although the presence and location of large Antarctic subglacial lakes at this time may remain challenging to appreciate, the process by which significant water loss may occur from them provides a mechanism that may be relevant to the Labyrinth’s formation.

Limitation of this study

In this study, the analysis of anomalous englacial stratigraphy above LSE is limited to information from available data, and in particular the lack of 3-D measurements of surface and basal boundary conditions has limited the complexity of the ice-flow model that we can apply. While estimates of these boundary conditions can be inferred from indirect measurements and modeling approaches, the absence of direct, high-resolution measurements, such as in-situ measurements of surface accumulation rate, is limiting. In a simple model, the intricate interplay among these boundary conditions can also introduce a trade-off effect, making it challenging to precisely evaluate the impact of each individual parameter choice in isolation. We employ a simplified 2.5D flowband model, because a 3D full-Stokes model, and especially a coupled lake-circulation model, would not be appropriately constrained in this study. A simplified modeling approach is also consistent with our goal, which is to prioritize the identification of first order causes for the observed englacial stratigraphic anomalies above LSE. However, more sophisticated models have been applied to subglacial lakes in problems where englacial stratigraphy is also evaluated. For example, Gudlaugsson and others (2016) used a 3-D full-Stokes ice-flow model to investigate lake drainage events. There are processes and complexities within the lake, as well as at the transition between grounded and floating ice, that we do not capture in our simplified approach. In particular, our steady state model does not fully reproduce the meters to tens of meters scale observed changes in surface slope and elevation upstream of LSE (Fig. S8 and S9), which are likely driven by changes in bed topography and/or basal conditions. This is worth investigating more in the future, especially if 3-D data become available. Future studies, incorporating additional direct measurements, have the potential to conduct a more comprehensive investigation into the dynamics and evolution of the system.

The complex topographic setting of the LSE area imposes challenges for the ice flow model used in this study (Fig. 1b, and Fig. 4a). The ice flow model assumes the Shallow-Ice Approximation (SIA) across the model domain except over the lake when it is active (Cuffey and Paterson, 2010). The simplicity of the model allows us to efficiently conduct a suite of experiments and isolate the influence of a smaller set of key parameter values. However, the model may not adequately account for local variations in the englacial velocity field induced by small-scale subglacial topographic features. LSE is located inside a subglacial canyon channel, whose main axis is oriented orthogonally to the local ice flow direction. The along-flow topographic relief of the canyon channel exceeds 1000 meters over just a few kilometers (Yan and others, 2022). Such extreme subglacial topographic relief can complicate the ice flow, and these 3-D effects are not adequately represented in the simple model used in this study. Consequently, the englacial velocity field in the model, particularly in regions closer to the ice-rock interface, may be misrepresented. This likely is the primary source of the persistent negative mismatch above the upstream canyon wall that is observed in all model runs (Fig. 5, Fig. 6, and Fig. S7). To address these limitations, future research can benefit from improved resolution of the subglacial topography, potentially through additional measurements and techniques such as geostatistical realization (e.g., MacKie and others, 2021). Moreover, incorporating more sophisticated modeling approaches (e.g., Shapero and others, 2021)—capable of better representing the strain and stress fields induced by extreme subglacial topographic relief—would enhance the accuracy of future simulations and reduce the observed mismatches.

We expect that the irregular layering in the vicinity of and across LSE has developed locally. Internal layers reflect the influence of surface and basal boundary conditions, both at the location where boundary conditions change and integrated along flow. While internal structure related to changes in boundary conditions can be advected downstream, this structure will become diffused unless spatial and/or temporal changes in boundary conditions persist. In our case, the transition in surface and basal conditions associated with lake initiation is a significant change in boundary conditions. We do not have evidence of upstream changes in boundary conditions that are like this, though they cannot be ruled out. Vieli and others (2007) provided some intuition about 3-D layer geometries resulting from changes in flow mode, though not specifically for a subglacial lake, which shows the most significant irregularities in layering very near to the location

where boundary conditions change. They discussed how layer shape may be affected downstream, but this was to a more muted degree. Our model domain extends from the upstream ice divide, where the ice flow originates, so the upstream influences on layer structure that are included in the model will be reflected in the stratigraphy at LSE.

In this study, we implemented a simplified assumption of homogeneous basal melt rate across the ice-water interface for LSE. In reality, basal melt and freezing rates are likely to vary due to factors such as lake circulation, spatial heterogeneities in geothermal heat flux, and local ice dynamics (e.g., Siegert, 2005; Filina and others, 2008). However, due to the current lack of reliable estimates for the lake's circulation patterns and the surrounding subglacial geological and hydrological conditions, it is difficult to estimate the spatial distribution of basal melting and freezing. Therefore, as an initial step towards understanding the basal melt pattern, we have assumed a homogeneous basal melt rate in this study. Future studies are encouraged to consider spatial variability in basal melting and freezing rates as more measurements and data become available.

We note that the satellite-measured ice flow velocity in the LSE area are often close to, or even below, the measurement uncertainty (Fig. 1 and Fig. 4) (Rignot and others, 2017). This introduces a significant limitation, as small-scale variations in ice flow speed and direction cannot be reliably resolved. Given the complex subglacial topography of the region, it is likely that such small-scale variations are prevalent. However, due to the inability to fully capture these variations through measurements, they are not well represented in our model. As a result, their potential imprint on englacial stratigraphy cannot be thoroughly investigated. Future in-situ measurements of ice flow velocity in this area will be very valuable for resolving these small-scale variations, allowing for a more accurate representation of their influence on englacial stratigraphy.

CONCLUSION

In this study, we map out the englacial radio-stratigraphy in the LSE area, where we observe a disruption of englacial stratigraphy above the lake, situated over an englacial reflection that is estimated to be around 12 kyr old. We use a 2.5-D ice flow model to investigate the first order causes for this stratigraphic disruption.

After comparing the model output using a suite of runs that evaluated 1404 different parameter combinations, our modeling results indicate changes in the production and transport of water in the wider catchment during the last glacial transition likely led to a significant increase in LSE water level and volume. This inference offers a rare insight into the sensitivity of a major Antarctic subglacial lake to the changes of climate and glacial conditions and underscores the impact that environmental changes can have on subglacial water bodies.

Previous studies have shown that subglacial lake water volumes can fluctuate on yearly-to-decadal time scales (e.g., Livingstone and others, 2022), where lakes are largely unconstrained by topography and are hence sensitive to relatively small glaciological changes, often dictated by the water volume itself (i.e. self-regulating). No large topographically-constrained subglacial lake has previously been shown to have experienced volume change. Our work reveals even large topographically-constrained lakes can experience volume change, not over years to decades due to small glaciological adjustments, but likely over centuries and due to major glaciological reconfigurations. This finding opens the possibility of water volume adjustments over glacial cycles to lake environments thought previously to be stable to external influences.

DATA AVAILABILITY STATEMENT

Ice thickness and bed elevation data of Princess Elizabeth Land, East Antarctica used in this study is from Cui and others (2020), which can be found at https://doi.org/10.5281/zenodo.4023343. The ice surface velocity used in this study is from MEaSUREs InSAR-Based Antarctic Ice Velocity Map, Version 2 (Rignot and others, 2017), which can be found at https://nsidc.org/data/nsidc-0484/versions/2. The englacial IRH picks done for this study can be found at https://doi.org/10.5281/zenodo.14962526. Original radargrams collected in the study area by ICECAP2 are available upon contacting the authors.

ACKNOWLEDGEMENTS

We are grateful for the generous financial, logistical, and technical support from: the G. Unger Vetlesen Foundation (New York, USA), University of Texas

Institute for Geophysics, the National Science Foundation Center for Oldest Ice Exploration (NSF COLDEX), the Antarctic Gateway Partnership (University of Tasmania, Australia), the University of Washington, the Polar Research Institute of China, the National Natural Science Foundation of China (grant 41876227), the Australian Antarctic Division, and the Global Innovation Initiative jointly funded by the U.S. Department of State and the UK Foreign Office. This work was in part supported by U.S. National Science Foundation grants 1443690 and OPP-2114454. We express our gratitude toward the expeditioners of the Chinese National Antarctic Research Expedition (CHINARE) 33rd and 34th field seasons and the Australian Antarctic Division–University of Texas Institute for Geophysics 4346/ICP10 field campaign. We thank S. Kempf, M. Wiederspahn and G. Ng for their assistance with data processing. We acknowledge support of this work by Landmark Software and Services, a Halliburton Company. We thank Prof. Neil Ross and two anonymous reviewers for reviewing this manuscript and providing valuable feedback that significantly improved the quality of this manuscript. We thank Dr. Dustin Schroeder and Prof. Frank Pattyn for their time and effort in overseeing the review process and editing this manuscript. This is UTIG contribution #4004.

REFERENCE:

Ashmore DW, Bingham RG, Ross N, Siegert MJ, Jordan TA and Mair DWF (2020) Englacial Architecture and Age-Depth Constraints Across the West Antarctic Ice Sheet. *Geophysical Research Letters* **47**(6), 1–11. doi:10.1029/2019GL086663.

Bazin L and others (2013) An optimized multi-proxy, multi-site Antarctic ice and gas orbital chronology (AICC2012): 120-800 ka. *Climate of the Past* **9**(4), 1715–1731. doi:10.5194/cp-9-1715-2013.

Beem LH and others (2018) Ice-flow reorganization within the East Antarctic Ice Sheet deep interior. *Geological Society Special Publication* **461**(1), 35–47. doi:10.1144/SP461.14.

Bingham RG and others (2024) Review Article: Antarctica’s internal architecture: Towards a radiostratigraphically-informed age–depth model of the Antarctic ice sheets. *EGUsphere*, 1–66. doi:10.5194/egusphere-2024-2593.

Carter SP and others (2011) Modeling 5 years of subglacial lake activity in the MacAyeal Ice Stream (Antarctica) catchment through assimilation of ICESat laser altimetry. *Journal of Glaciology* **57**(206), 1098–1112. doi:10.3189/002214311798843421.

Cavitte M and others (2021) A detailed radiostratigraphic data set for the central East Antarctic Plateau spanning from the Holocene to the mid-Pleistocene Marie. *Earth System Science Data Discussions* **13**, 4759–4777. doi:10.5194/essd-2020-393.

Cavitte MGP and others (2018) Accumulation patterns around Dome C, East Antarctica, in the last 73 kyr. *Cryosphere* **12**(4), 1401–1414. doi:10.5194/tc-12-1401-2018.

Cavitte MGP and others (2016) Deep radiostratigraphy of the East Antarctic plateau: Connecting the Dome C and Vostok ice core sites. *Journal of Glaciology* **62**(232), 323–334. doi:10.1017/jog.2016.11.

Cuffey KM and Paterson WSB (2010) *The Physics of Glaciers, 4th edition.* Butterworth-Heinemann, Elsevier.

Cui X and others (2020) Bed topography of Princess Elizabeth Land in East Antarctica. *Earth System Science Data* **12**(4), 2765–2774. doi:10.5194/essd-12-2765-2020.

Cui X and others (2018) The First Fixed-wing Aircraft for Chinese Antarctic Expeditions: Airframe, modifications, Scientific Instrumentation and Applications. *Journal of Environmental and Engineering Geophysics* **23**(1), 1–13. doi:10.2113/JEEG23.1.1.

Dansgaard W and Johnsen SJ (1969) A flow model and a time scale for the ice core from Camp Century , Greenland. *Journal of Glaciology* **8**, 215–223.

Das I and others (2013) Influence of persistent wind scour on the surface mass balance of Antarctica. *Nature Geoscience* **6**(5), 367–371. doi:10.1038/ngeo1766.

Denton GH and Sugden DE (2005) Meltwater features that suggest miocene ice-sheet overriding of the transantarctic mountains in victoria land, antarctica. *Geografiska Annaler: Series A, Physical Geography* **87**(1), 67–85. doi:10.1111/j.0435-3676.2005.00245.x.

Dowdeswell JA and Siegert MJ (1999) The dimensions and topographic setting of Antarctic subglacial lakes and implications for large-scale water storage beneath continental ice sheets. *Bulletin of the Geological Society of America* **111**(2), 254–263. doi:10.1130/0016-7606(1999)111<0254:TDATSO>2.3.CO;2.

Eisen O, Wilhelms F, Steinhage D and Schwander J (2006) Improved method to determine radio-echo sounding reflector depths from ice-core profiles of permittivity and conductivity. *Journal of Glaciology* **52**(177), 299–310. doi:10.3189/172756506781828674.

Elsworth CW, Schroeder DM and Siegfried MR (2020) Interpreting englacial layer deformation in the presence of complex ice flow history with synthetic radargrams. *Annals of Glaciology* **61**(81), 206–213. doi:10.1017/aog.2019.41.

Filina IY, Blankenship DD, Thoma M, Lukin VV, Masolov VN and Sen MK (2008) New 3D bathymetry and sediment distribution in Lake Vostok: Implication for pre-glacial origin and numerical modeling of the internal processes within the lake. *Earth and Planetary Science Letters* **276**(1–2), 106–114. doi:10.1016/j.epsl.2008.09.012.

Frémand AC and others (2023) Antarctic Bedmap data: Findable, Accessible, Interoperable, and Reusable (FAIR) sharing of 60 years of ice bed, surface, and thickness data. *Earth System Science Data* **15**(7), 2695–2710. doi:10.5194/essd-15-2695-2023.

Fricker HA, Siegfried MR, Carter SP and Scambos TA (2016) A decade of progress in observing and modelling Antarctic subglacial water systems. *Philosophical Transactions of the Royal Society A: Mathematical, Physical and Engineering Sciences* **374**(2059), 20140294. doi:10.1098/rsta.2014.0294.

Fricker HA, Scambos T, Bindschadler R and Padman L (2007) An active subglacial water system in West Antarctica mapped from space. *Science* **315**(5818), 1544–1548. doi:10.1126/science.1136897.

Gowan EJ and others (2021) A new global ice sheet reconstruction for the past 80000 years. *Nature Communications* **12**(1199), 1–9. doi:10.1038/s41467-021-21469-w.

Grima C, Blankenship DD, Young DA and Schroeder DM (2014) Surface slope control on firn density at Thwaites Glacier, West Antarctica: Results from airborne radar sounding. *Geophysical Research Letters* **41**(19), 6787–6794. doi:10.1002/2014GL061635.

Gudlaugsson E, Humbert A, Kleiner T, Kohler J and Andreassen K (2016) The influence of a model subglacial lake on ice dynamics and internal layering. *The Cryosphere* **10**(2), 751–760. doi:10.5194/tc-10-751-2016.

Gudmundsson GH (2011) Inverse Methods in Glaciology. Singh VP, Singh P, and Haritashya UK eds. *Encyclopedia of Snow, Ice and Glaciers*. Springer Netherlands, Dordrecht, 653–656. doi:10.1007/978-90-481-2642-2_648.

Guo J and others (2020) Historical surface mass balance from a frequency-modulated continuous-wave (FMCW) radar survey from Zhongshan station to Dome A. *Journal of Glaciology* **66**(260), 965–977. doi:10.1017/jog.2020.58.

Gustafson CD and others (2022) A dynamic saline groundwater system mapped beneath an Antarctic ice stream. *Science* **376**(6593), 640–644. doi:10.1126/science.abm3301.

Jamieson SSR and others (2016) An extensive subglacial lake and canyon system in Princess Elizabeth Land, East Antarctica. *Geology* **44**(2), 87–90. doi:10.1130/G37220.1.

Jezek KC, Curlander JC, Carsey F, Wales C and Barry. RG (2013) RAMP AMM-1 SAR Image Mosaic of Antarctica, Version 2. *Boulder, Colorado USA. NASA National Snow and Ice Data Center Distributed Active Archive Center*. doi:https://doi.org/10.5067/8AF4ZRPULS4H. Date Accessed 11-07-2022.

Kennicutt MC and others (2019) Sustained Antarctic Research: A 21st Century Imperative. *One Earth* **1**(1), 95–113. doi:10.1016/j.oneear.2019.08.014.

Koutnik MR and others (2016) Holocene accumulation and ice flow near the West Antarctic Ice Sheet Divide ice core site. *Journal of Geophysical Research: Earth Surface* **121**(5), 907–924. doi:10.1002/2015JF003668.

Koutnik MR and Waddington ED (2012) Well-posed boundary conditions for limited-domain models of transient ice flow near an ice divide. *Journal of Glaciology* **58**(211), 1008–1020. doi:10.3189/2012JoG11J212.

Leysinger Vieli GJ-MC, Martín C, Hindmarsh RCA and Lüthi MP (2018) Basal freeze-on generates complex ice-sheet stratigraphy. *Nature Communications* **9**(1), 4669. doi:10.1038/s41467-018-07083-3.

Leysinger Vieli GJ-MC, Hindmarsh RCA, Siegert MJ and Bo S (2011) Time-dependence of the spatial pattern of accumulation rate in East Antarctica deduced from isochronic radar layers using a 3-D numerical ice flow model. *Journal of Geophysical Research: Earth Surface* **116**(F2). doi:10.1029/2010JF001785.

Li L, Aitken ARA, Lindsay MD and Kulessa B (2022) Sedimentary basins reduce stability of Antarctic ice streams through groundwater feedbacks. *Nature Geoscience* **15**(August). doi:10.1038/s41561-022-00992-5.

Livingstone SJ and others (2022) Subglacial lakes and their changing role in a warming climate. *Nature reviews Earth & EnvironmEnt*. doi:10.1038/s43017-021-00246-9.

MacKie EJ, Schroeder DM, Zuo C, Yin Z and Caers J (2021) Stochastic modeling of subglacial topography exposes uncertainty in water routing at Jakobshavn Glacier. *Journal of Glaciology* **67**(261), 75–83. doi:10.1017/jog.2020.84.

Maule CF, Purucker ME, Olsen N and Mosegaard K (2005) Geophysics: Heat flux anomalies in Antarctica revealed by satellite magnetic data. *Science* **309**(5733), 464–467. doi:10.1126/science.1106888.

Pelle T, Greenbaum JS, Dow CF, Jenkins A and Morlighem M (2023) Subglacial discharge accelerates future retreat of Denman and Scott Glaciers, East Antarctica. *Science Advances* **9**(43), eadi9014. doi:10.1126/sciadv.adi9014.

Peters ME, Blankenship DD, Carter SP, Kempf SD, Young DA and Holt JW (2007) Along-track focusing of airborne radar sounding data from west antarctica for improving basal reflection analysis and layer detection. *IEEE Transactions on Geoscience and Remote Sensing* **45**(9), 2725–2736. doi:10.1109/TGRS.2007.897416.

Peters ME, Blankenship DD and Morse DL (2005) Analysis techniques for coherent airborne radar sounding: Application to West Antarctic ice streams. *Journal of Geophysical Research: Solid Earth* **110**(6), 1–17. doi:10.1029/2004JB003222.

Rignot E, Mouginot J and Scheuchl B (2017) MEaSUREs InSAR-Based Antarctica Ice Velocity Map, Version 2. *Boulder, Colorado USA. NASA National Snow and Ice Data Center Distributed Active Archive Center*. doi:https://doi.org/10.5067/D7GK8F5J8M8R.

Ross N and Siegert M (2020) Basal melting over Subglacial Lake Ellsworth and its catchment: Insights from englacial layering. *Annals of Glaciology* **61**(81), 198–205. doi:10.1017/aog.2020.50.

Schroeder DM and others (2020) Five decades of radioglaciology. *Annals of Glaciology* **61**(81), 1–13. doi:10.1017/aog.2020.11.

Schroeder DM, Blankenship DD and Young DA (2013) Evidence for a water system transition beneath thwaites glacier, West Antarctica. *Proceedings of the National Academy of Sciences of the United States of America* **110**(30), 12225–12228. doi:10.1073/pnas.1302828110.

Sergienko OV and Hulbe CL (2011) 'Sticky spots' and subglacial lakes under ice streams of the Siple Coast, Antarctica. *Annals of Glaciology* **52**(58), 18–22. doi:10.3189/172756411797252176.

Shackleton C, Matsuoka K, Moholdt G, Van Liefferinge B and Paden J (2023) Stochastic Simulations of Bed Topography Constrain Geothermal Heat Flow and Subglacial Drainage Near Dome Fuji, East Antarctica. *Journal of Geophysical Research: Earth Surface* **128**(11), e2023JF007269. doi:10.1029/2023JF007269.

Shapero DR, Badgeley JA, Hoffman AO and Joughin IR (2021) icepack: a new glacier flow modeling package in Python, version 1.0. *Geoscientific Model Development* **14**(7), 4593–4616. doi:10.5194/gmd-14-4593-2021.

Siegert MJ and others (2014) Boundary conditions of an active West Antarctic subglacial lake: implications for storage of water beneath the ice sheet. *The Cryosphere* **8**(1), 15–24. doi:10.5194/tc-8-15-2014.

Siegert MJ (2005) LAKES BENEATH THE ICE SHEET: The Occurrence, Analysis, and Future Exploration of Lake Vostok and Other Antarctic Subglacial Lakes. *Annual Review of Earth and Planetary Sciences* **33**(1), 215–245. doi:10.1146/annurev.earth.33.092203.122725.

Siegert MJ and others (2004) Ice Flow Direction Change in Interior West Antarctica. *Science* **305**(5692), 1948–1951. doi:10.1126/science.1101072.

Siegert MJ, Kwok R, Mayer C and Hubbard B (2000) Water exchange between the subglacial Lake Vestok and the overlying ice sheet. *Nature* **403**(6770), 643–646. doi:10.1038/35001049.

Siegfried MR and others (2023) The life and death of a subglacial lake in West Antarctica. *Geology*. doi:10.1130/G50995.1.

Smith AM and others (2018) Evidence for the long-term sedimentary environment in an Antarctic subglacial lake. *Earth and Planetary Science Letters* **504**, 139–151. doi:10.1016/j.epsl.2018.10.011.

Sugiyama S and others (2012) Snow density along the route traversed by the Japanese-Swedish Antarctic Expedition 2007/08. *Journal of Glaciology* **58**(209), 529–539. doi:10.3189/2012JoG11J201.

Thoma M, Grosfeld K, Filina I and Mayer C (2009) Modelling flow and accreted ice in subglacial Lake Concordia, Antarctica. *Earth and Planetary Science Letters* **286**(1), 278–284. doi:10.1016/j.epsl.2009.06.037.

Veres D and others (2013) The Antarctic ice core chronology (AICC2012): an optimized multi-parameter and multi-site dating approach for the last 120 thousand years. *Climate of the Past* **9**(4), 1733–1748. doi:10.5194/cp-9-1733-2013.

Verfaillie D and others (2012) Snow accumulation variability derived from radar and firn core data along a 600 km transect in Adelie Land, East Antarctic plateau. *The Cryosphere* **6**(6), 1345–1358. doi:10.5194/tc-6-1345-2012.

Vieli GJ-MCL, Hindmarsh RCA and Siegert MJ (2007) Three-dimensional flow influences on radar layer stratigraphy. *Annals of Glaciology* **46**, 22–28. doi:10.3189/172756407782871729.

Waddington ED, Neumann TA, Koutnik MR, Marshall HP and Morse DL (2007) Inference of accumulation-rate patterns from deep layers in glaciers and ice sheets. *Journal of Glaciology* **53**(183), 694–712. doi:10.3189/002214307784409351.

Wei W and others (2019) Getz Ice Shelf melt enhanced by freshwater discharge from beneath the West Antarctic Ice Sheet. *The Cryosphere Discussions*, 1–16. doi:10.5194/tc-2019-170.

van Wessem JM and others (2018) Modelling the climate and surface mass balance of polar ice sheets using RACMO2 – Part 2: Antarctica (1979–2016). *The Cryosphere* **12**(4), 1479–1498. doi:10.5194/tc-12-1479-2018.

Wingham DJ, Siegert MJ, Shepherd A and Muir AS (2006) Rapid discharge connects Antarctic subglacial lakes. *Nature* **440**(7087), 1033–1036. doi:10.1038/nature04660.

Wright AP, Siegert MJ, Le Brocq AM and Gore DB (2008) High sensitivity of subglacial hydrological pathways in Antarctica to small ice-sheet changes. *Geophysical Research Letters* **35**(17), 1–5. doi:10.1029/2008GL034937.

Wright A and Siegert MJ (2011) The identification and physiographical setting of Antarctic subglacial lakes: An update based on recent discoveries. Siegert MJ, Kennicutt MC, and Bindschadler RA eds. *Geophysical Monograph Series*. American Geophysical Union, Washington, D. C., 9–26. doi:10.1029/2010GM000933.

Wrona T, Wolovick MJ, Ferraccioli F, Corr H, Jordan T and Siegert MJ (2018) Position and variability of complex structures in the central East Antarctic Ice Sheet. *Geological Society Special Publication* **461**(1), 113–129. doi:10.1144/SP461.12.

Yan S and others (2022) A newly discovered subglacial lake in East Antarctica likely hosts a valuable sedimentary record of ice and climate change. *Geology* **50(8)**, 949–953. doi:https://doi.org/10.1130/G50009.1.

Young DA and others (2017) High-resolution boundary conditions of an old ice target near Dome C, Antarctica. *The Cryosphere* **11**(4), 1897–1911. doi:10.5194/tc-11-1897-2017.

Young DA and others (2011) A dynamic early East Antarctic Ice Sheet suggested by ice-covered fjord landscapes. *Nature* **474**(7349), 72–75. doi:10.1038/nature10114.

Zwally HJ, Giovinetto MB, Beckley MA and Saba JL (2012) Antarctic and Greenland Drainage Systems.

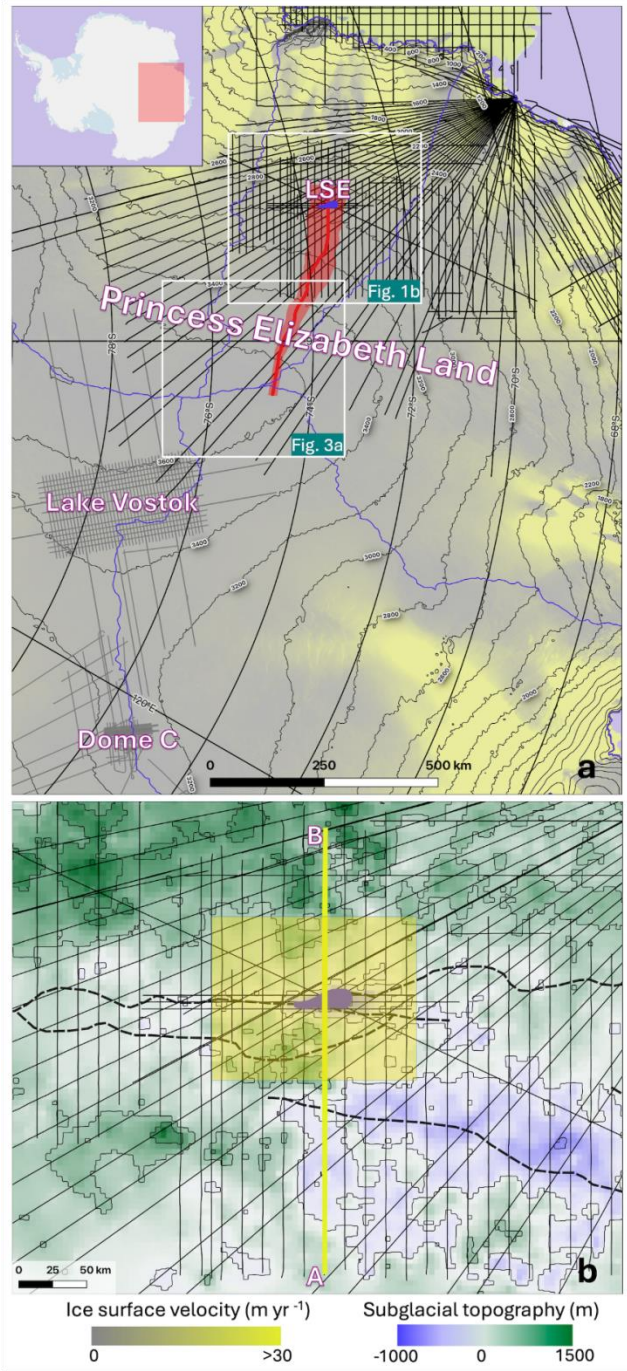

Fig. 1. Map of the study area. a: Surface elevation and velocity map. The background color shows the ice flow speed from MEaSUREs InSAR-Based Antarctic Ice Velocity Map, Version 2 (Rignot and others, 2017). Blue lines mark the location of ice divides (Zwally and others, 2012). Surface elevation contours are shown in thick gray lines (Jezek and others, 2013). The red line marks the location of the flowline used for the ice flow model, while the red shade marks the

flowband width, both based on the surface velocity data from MEaSUREs InSAR-Based Antarctic Ice Velocity Map, Version 2 (Rignot and others, 2017). Black lines show the location of airborne geophysical survey collected in Princess Elizabeth Land (Cui and others, 2020), while thin gray lines show the location of pre-existing airborne geophysical dataset in the Lake Vostok and Dome C areas (Young and others, 2017; Frémand and others, 2023). The location of LSE is marked by the blue area (Yan and others, 2022). The map at up-left shows the overall location of this map. The location of panel b and Fig. 3a are marked by white rectangles. b: Subglacial topography of the LSE area. The background color shows the subglacial topography of the LSE area, as measured by airborne radio-echo sounding survey (Cui and others, 2020). Subglacial topography contour has intervals of 250 meters (thin) and 1000 meters (thick). The black lines show the location of the airborne geophysics survey collected in the area through the ICECAP2 initiative (Cui and others, 2020). The location of LSE is marked by the blue area (Yan and others, 2022). Thick blue dash line shows the location of the subglacial canyon network, estimated from satellite-based remote-sensing (Jamieson and others, 2016). The thick yellow line highlights the location of the radargram shown in Fig. 2. The yellow square marks the location of the map shown in Fig. 4.

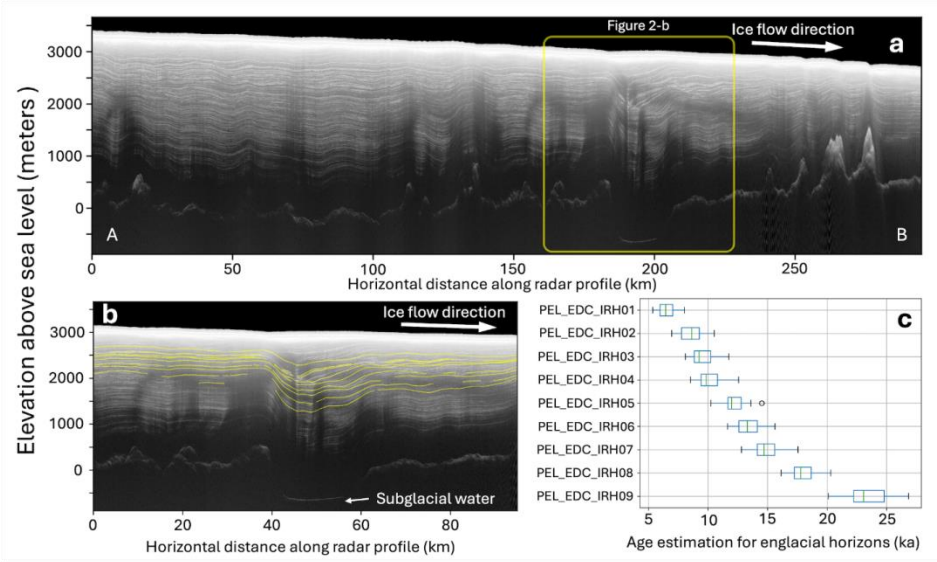

Fig. 2. Englacial radio-stratigraphy above LSE. a: Example radargram collected through the LSE area. The location and orientation of this radargram is marked in Fig. 1. Additional radargrams collected through the LSE area can be found in the Supplementary Materials (Fig. S1 and Fig. S2). b: A zoom-in view of the stratigraphic disruption above LSE, whose location is marked in panel a. Yellow lines show the nine traced englacial reflections in the LSE area, with PEL_EDC_IRH01 being the shallowest (closest to the ice surface) and PEL_EDC_IRH09 being the deepest. c: Age estimation of the nine traced englacial reflections in the LSE area. All elevation data shown in this manuscript are relative to the WGS84 ellipsoid.

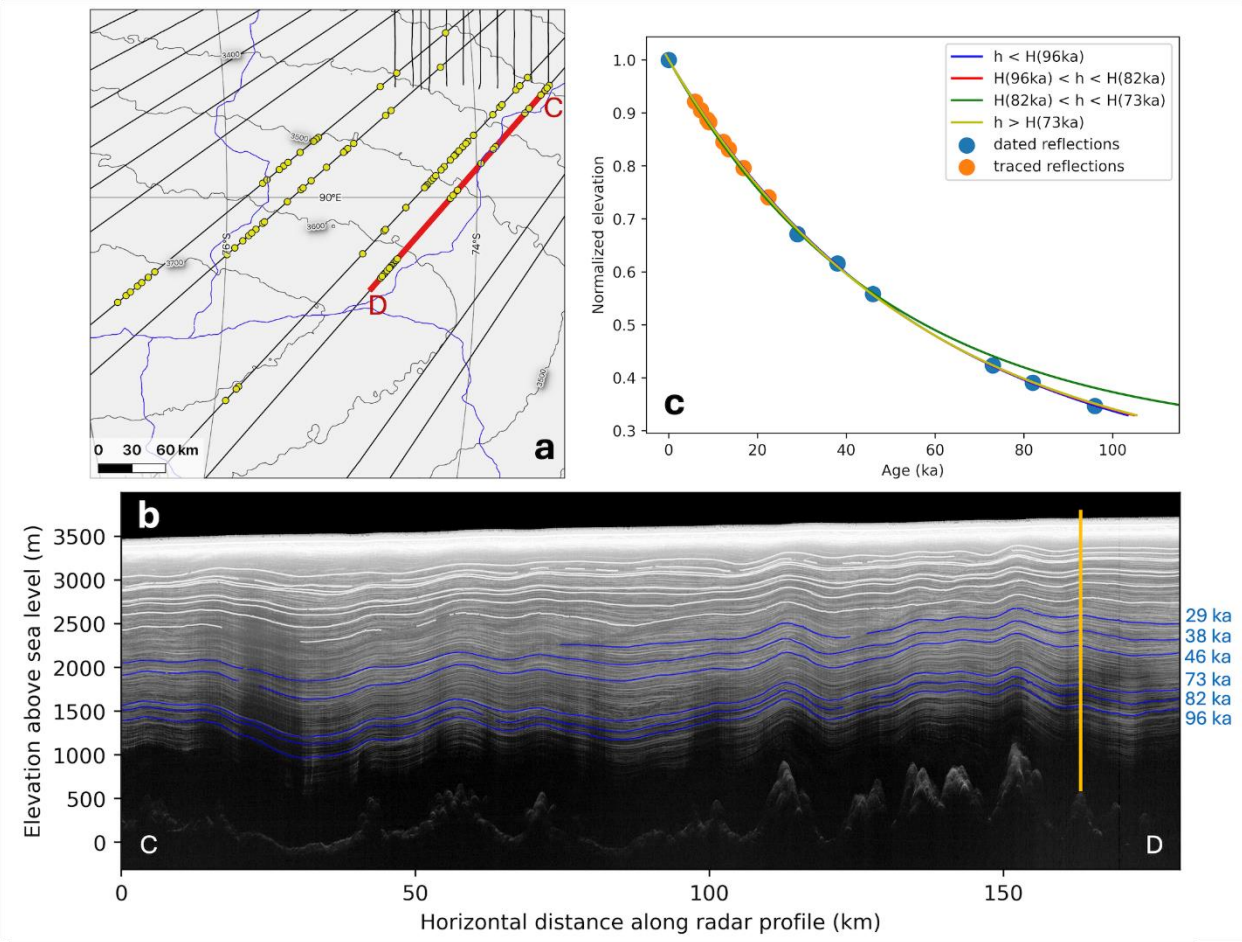

Fig. 3. Age estimation of traced IRHs. a: A map of interior PEL, whose location is marked in Fig. 1a. Black lines show the airborne radar transects collected by ICECAP2. Yellow dots show the 91 locations where the Dansgaard-Johnsen model is used to constrain the age-depth profile. Red line highlights the location and orientation of the radargram shown in panel b. Blue lines mark the location of ice divides (Zwally and others, 2012). Surface elevation contours are shown in thick gray lines (Jezek and others, 2013). b: An example radargram showing the nine undated IRHs traced for the LSE area (white lines) and the six dated IRHs extended from the Dome C area (blue lines, ages are mark on the right-hand side). c: A comparison between the age-depth curves derived from different assumptions of the basal shear layer thickness (h) at the same location, whose location is marked by the yellow vertical bar in panel b. H represent the thickness between a certain IRH and the bedrock.

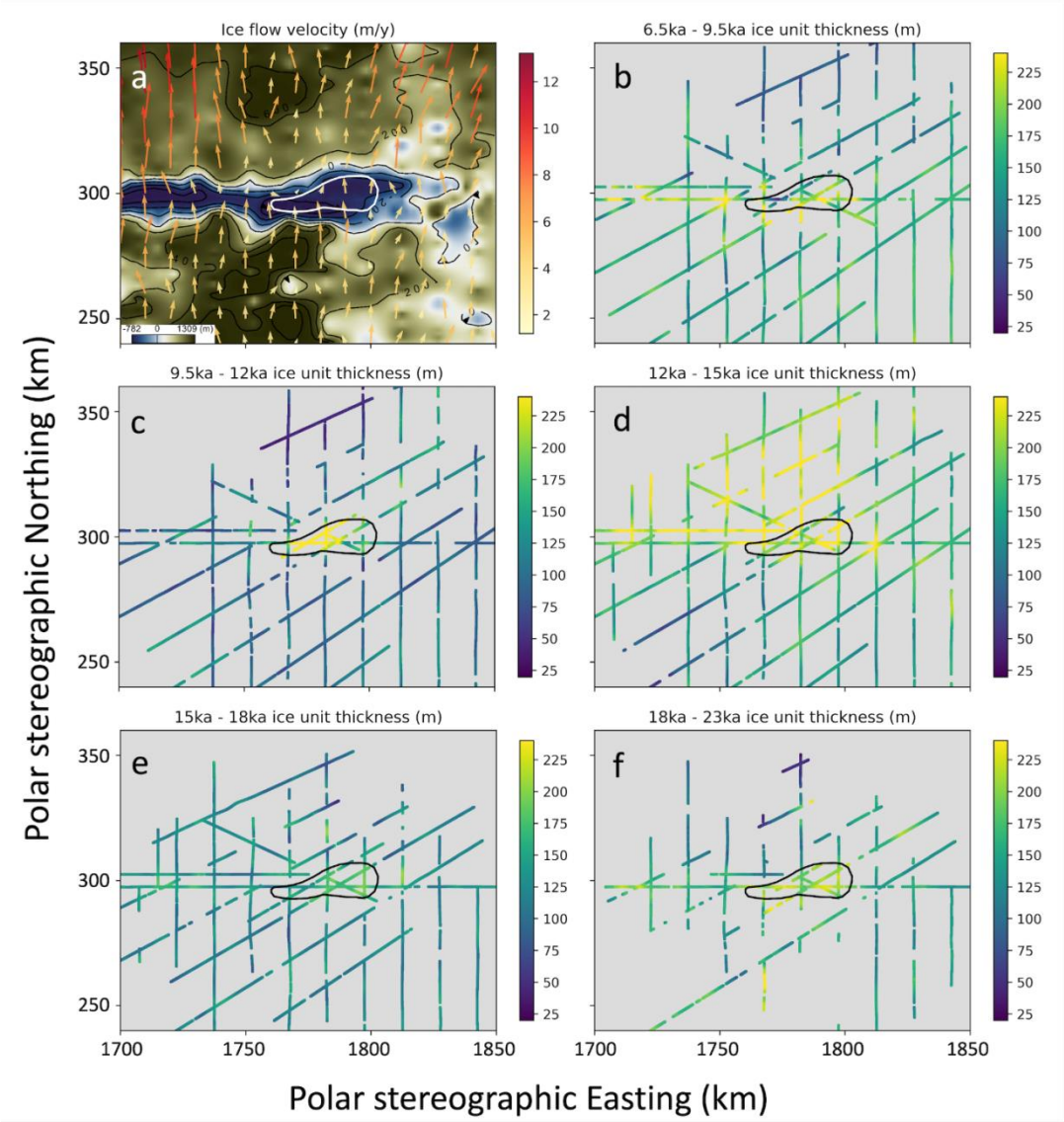

Fig. 4. a: Ice flow velocity (Rignot and others, 2017) in the LSE area plotted on a map of radar-derived subglacial topography (Cui and others, 2020). Subglacial LSE is shown by a white polygon line. Arrow direction represents ice flow direction, and arrow color and length represent ice flow rate. b-f: Thickness of ice layer unit between englacial reflections of specific ages. The age for each ice unit is labeled in subplot titles. Colorbar shows the layer packet thickness in meters. Subglacial LSE is shown by a black polygon line. Coordinates are in EPSG 3031–WGS 84 / Antarctic Polar Stereographic.

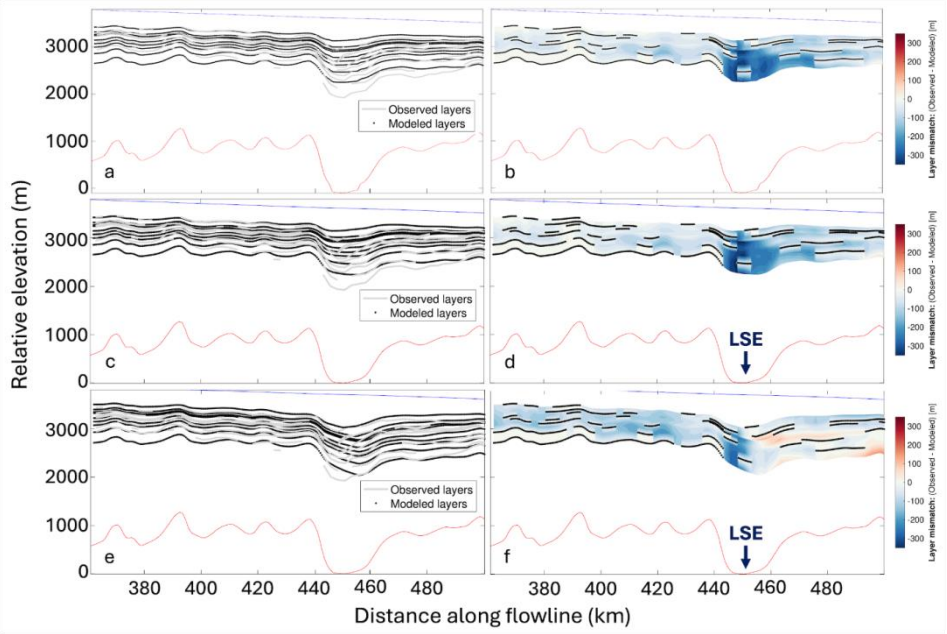

Fig. 5. Comparison of the observed and modeled IRHs from different model setups. a, c and e show direct comparisons between the modeled and observed IRHs depth, while b, d and f show the mismatch contour. Panel a and b are from the base run setup. Panel c and d are from the model setup with plug flow and basal melting. Panel e and f are from the model setup with surface snow redistribution. Please note that for the base run, we assume no waterfill in the LSE basin and drop the ice bottom for 100 meters, which is about the average water depth as estimated by Yan and others, (2020). The location of LSE is marked in d and f. For the mismatch contour plots, blue color means that the observed IRH is deeper than the modeled IRH, and black dots mark the discretized modeled IRHs depth where the traced IRHs depth is absent.

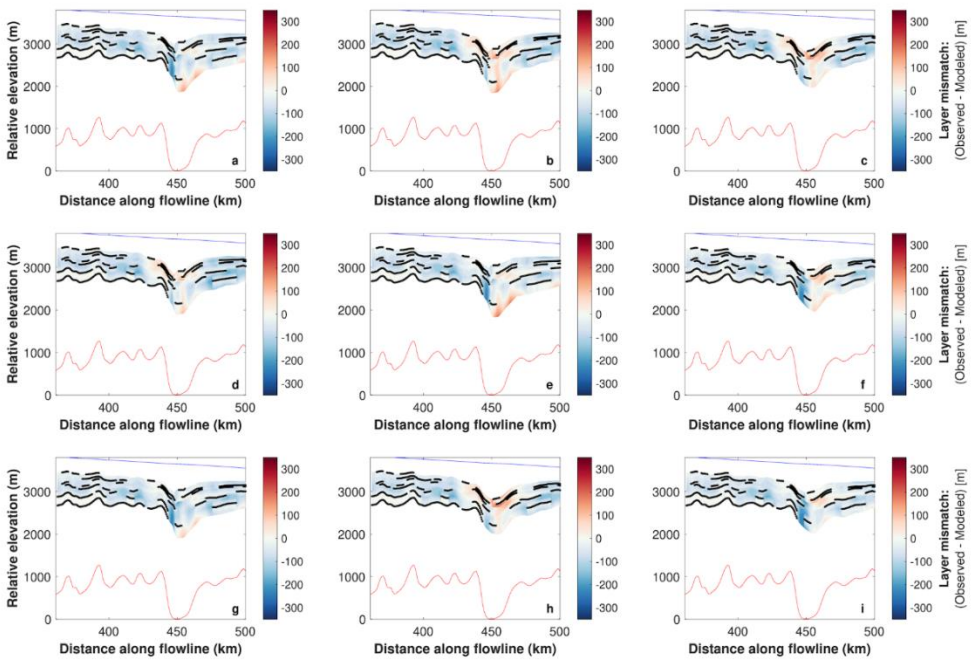

Fig. 6. Contour visualization of the 9 model setups that produce the best matches with the observed englacial stratigraphy among the 1404 tested setups. For the purpose of keeping figures concise, we show the 9 accepted setups with the smallest mismatch RMS here, with their parameters value listed in Table 3. The mismatch from the other 12 accepted setups is shown in Fig. S7 in the supplementary material, with their parameter combinations listed in Table S1 in the supplementary material. Blue color means that the observed IRH is deeper than the modeled IRH, and black dots show the modeled IRHs depth where the traced IRHs depth is absent.

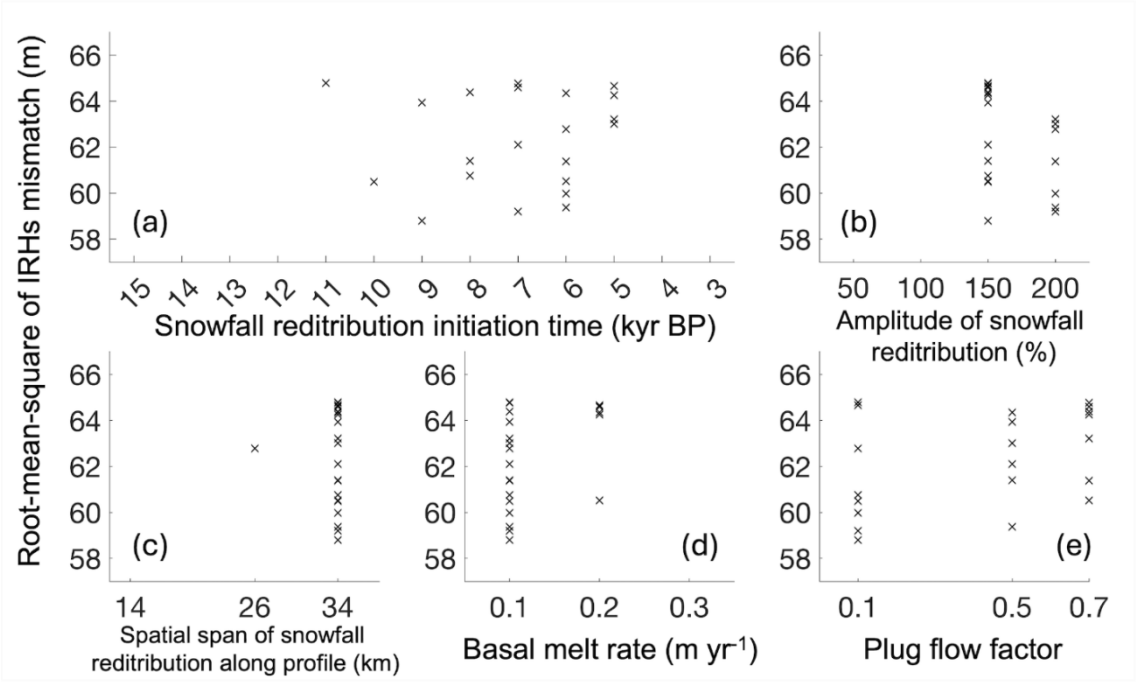

Fig. 7. Statistics of the tunable parameter values for the 21 model setups with RMS mismatch less than 65 meters.

Table 1. Statistics of age estimation for the traced IRHs in the LSE area. Errors reflect the standard deviation of the Dansgaard-Johnsen model results.

Traced IRH	Estimated age
PEL_EDC_IRH01	6.5 ± 0.6 kyrs
PEL_EDC_IRH02	8.5 ± 0.9 kyrs
PEL_EDC_IRH03	9.5 ± 0.8 kyrs
PEL_EDC_IRH04	10 ± 0.8 kyrs
PEL_EDC_IRH05	12 ± 0.8 kyrs
PEL_EDC_IRH06	13.5 ± 0.9 kyrs
PEL_EDC_IRH07	15 ± 1.0 kyrs
PEL_EDC_IRH08	18 ± 0.9 kyrs
PEL_EDC_IRH09	23.5 ± 1.7 kyrs

Table 2. Tunable parameters that affect the model outcome, and the estimated value ranges for each parameter that is searched through by a series of model runs.

Parameter	Value range
Time duration of snowfall redistribution	3 ka -15 ka, with 1 kyr stepping
Amplitude of snowfall redistribution	50%, 100%, 150%, 200%
Spatial span of surface snowfall redistribution along the model profile	14 km, 24km, 34 km
Basal melt rate over the lake	10 cm yr^{-1}, 20 cm yr^{-1}, 30 cm yr^{-1}
Plug flow velocity factor over the lake	0.1, 0.5, 0.7

Table 3. Parameters setup for the 9 runs with the smallest mismatch RMS values. The mismatch contour produced by the model setups listed here are shown in Fig. 6.

Run index as shown in Fig. 6	Time duration of snowfall redistribution (kyr)	Surface accumulation increase percentage	Surface accumulation increase span (km)	Basal melt rate (m yr^{-1})	Plug flow velocity factor	Mismatch RMS (m)
a	9	150%	34	0.1	0.1	59
b	7	200%	34	0.1	0.1	59
c	6	200%	34	0.1	0.5	59
d	6	200%	34	0.1	0.1	60
e	10	150%	34	0.1	0.1	60
f	6	150%	34	0.1	0.7	61
g	8	150%	34	0.1	0.1	61
h	6	200%	34	0.1	0.7	61
i	8	150%	34	0.1	0.5	61